The proposed inversion technique of remote sensing data for reservoir monitoring.

M. Yusup Nur Khakim[1][2], Takeshi Tsuji[1], and Toshifumi Matsuoka[1]

[1] *Kyoto University, Graduate School of Engineering* [2] *Sriwijaya University, Physics Dept.*

ABSTRACT

A map of ground surface deformations due to the geomechanical instability of the reservoir has been estimated by using a differential InSAR stacking technique. The surface deformations have valuable information about the dynamic reservoir and are most likely to occur in the production of hydrocarbon even if the reservoir is kilometers deep. In order to invert surface deformations obtained from InSAR data, we propose a two-step inversion approach based on a tensional rectangular dislocation model. The first step, we use genetic algorithms to estimate the depth and the geometry of reservoir deformation. However, this model provides a single dislocation with uniform deformation. This uniform deformation can not provide an adequate representation of the spatially varying deformation in the reservoir. Therefore, in the second step, we have applied the least square inversion with the penalty function and smoothing factor in order to efficiently invert the spatial distribution of reservoir deformations and volume changes from the surface deformation data. Through a synthetic model, we have examined our inversion approach by estimating the root mean square error and the relative error, then applied to real data. We conclude that the InSAR technology is useful to provide ground surface deformations and accurately monitor reservoir deformation using inversion techniques.

.

KEY WORDS: Monitoring, reservoir, deformation, inversion

INTRODUCTION

Teatini et al. (2011) presented the fundamental geomechanical processes that govern land uplift due to fluid injection in the subsurface for a variety of purposes, e.g. to enhanced oil recovery (EOR), store gas in depleted gas/oil fields, recharge overdrafted aquifer system (ASR), and mitigate anthropogenic land subsidence. The largest uplift depends on a number of factors, including the pore-fluid pressure increase, the depth, thickness and areal extent of the pressurized and heated geological formation.

A modern geodetic method, Synthetic Aperture Radar Interferometry (InSAR) technology, provides its capability for imaging the ground surface deformations over large area with small (1 cm or less) surface changes in all weather conditions (Burgmann et al., 2000). Klees and Massonnet (1999) discussed the potential applications of InSAR for the monitoring of deformations related to earthquake and crustal studies, the monitoring of volcanoes and anthropogenic effects, and the monitoring of glaciers and ice sheets. Meanwhile, some examples where surface deformation monitoring using InSAR due to fluid injection were carried out include the Belridge and Lost Hills fields in California (Patzek and Silin, 2000; Patzek et al., 2001) and the CO_2 sequestration at Krechba Algeria (Mathieson et al., 2009).

Because the surface uplift can be induced by reservoir expansion, the surface uplift has valuable information about the dynamic reservoir and it is most likely to occur in the production of hydrocarbon even if the reservoir is kilometers deep. Characterization of the surface deformation sources based on the InSAR measurements has therefore become major importance in reservoir monitoring activity, such as EOR, carbon capture and storage (CCS) project. The amplitude and the rate of surface deformation are key parameters to optimize economical production and to minimize environmental impact. One of the most common applications of these measurements is to numerically or analytically simulate the source of deformation.

In this study, we propose a two-step inversion from the surface uplift map obtained by InSAR measurement to estimate the distribution of reservoir deformations and reservoir volume change rates where the oil sand reservoir is undergoing steam injection, Steam Assisted Gravity Drainage (SAGD). In the first step, we estimate the geometry of reservoir deformation by inverting the uplift map measured by InSAR adopting Okada source model (Okada 1985) using genetic algorithm (GA) inversion. In the second step, we use least square method to obtain reservoir deformation thus reservoir volume changes can then be calculated. So far, this approach has not yet been presented in literatures for such case.

METHODOLOGY

Ground surface uplift derived from InSAR provides an excellent opportunity to analyze physical processes of steam chamber development in oil sand reservoirs. In order to invert the InSAR data, we adopted an elastic, homogeneous, and isotropic half-space with tensile dislocation plane movements. Appling Okada's

formula (Okada 1985) to this tensile dislocation model, we can evaluate the surface displacements. This formula is non-linear and characterized by a large number of parameters. Also this formula is frequently used in the characterization of earthquake faults. In this study, we applied the inversion technique to synthetic data and real one of an oil sand field under SAGD.

A main idea of our approach is in the first step to emphasize resolving accurately the depth of deformation source by means of GA inversion. A disadvantage using a uniform deformation approach is that the specific dislocation geometry may not provide an adequate representation of the spatially varying reservoir deformation. Therefore, in the first step of our approach, the reservoir deformation is roughly estimated. We then make use of the estimated depth of deformation source as a constraint in the second step by using least square inversion in order to improve the knowledge of the horizontal distribution of reservoir deformation and reservoir volume changes as well.

APPLICATIONS

SYNTHETIC MODEL

In order to examine the performance of the proposed two-step inversion technique, GA and least square inversion, we prepared a synthetic model of the distribution of reservoir deformation with magnitudes between 1 cm and 4 cm instead of a single dislocation with uniform deformation (Figure 1a). A volume change due to the deformation field in this model is 7.36×10^4 m^3. The synthetic model extends 2200 m long from east to west and 1600 m wide from north to south with a strike of N90°W. From this synthetic model, we applied forward modeling based on Okada's formula to obtain a synthetic uplift map (Figure 1b) and then added a gaussian noise with mean 0.0 and standard deviation 0.1 cm to the synthetic uplift map in order to generate a map of noisy synthetic uplift (Figure 1d) as an inversion input.

Using random initial models, we initially applied GA inversion to the synthetic uplift map (Figure 1d) in order to resolve model parameters. We evaluated individual of solutions by means of misfit between the observed and calculated surface uplift. The best solution from the evaluation of 500 generations has the least misfit of the solution 0.0324 (the fitness of 96.76%). In order to measure the accuracy of the solutions, we also calculated the root mean square errors (RMSE) of the best solution 0.23 cm due to the presence of the additive noise. A relative error of the depth with the range of space search between 100 m and 600 m is 0.2%. In addition, the relative error of a uniform deformation over reservoir is 23.4%.
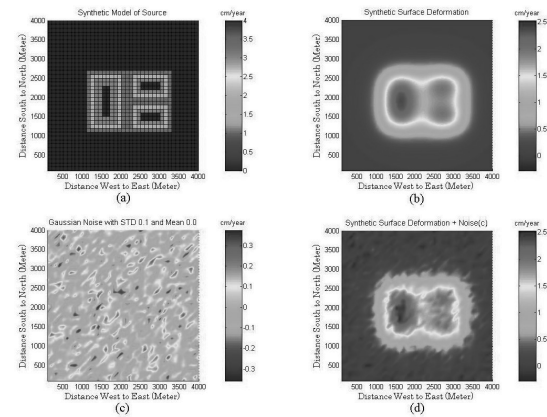

Figure 1. (a) Synthetic model of reservoir deformations, (b) synthetic surface uplift resulting forward modeling, (c) additive noise, and (d) synthetic surface uplift with additive noise
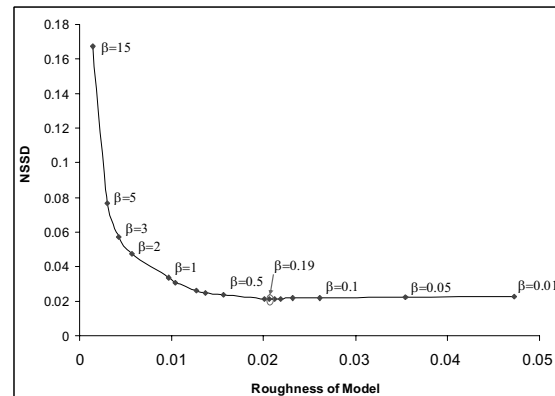

Figure 2. Trade-off curve between roughness and NSSD of solution for synthetic data.

In order to improve the solution of reservoir deformations from homogeneous into heterogeneous fields, we applied the least square technique in the second step of the proposed inversion. The deformation distributions should become more realistic and produce good fit the model. In this step, the ground surface and reservoir of the synthetic model are divided into 40 rectangular elements in W-E and S-N directions. Therefore, there are 1600 elements on the surface and in the reservoir and each gridded element is 100 m in length and in width. We used a penalty function with smoothing factors (β) in this least square inversion in order to search for the optimum distribution of reservoir deformation. From the larger smoothing factor, we obtained the smoother vertical reservoir deformation. However, normalized sum-squared differences (NSSD) become larger. Therefore, we needed to investigate a trade-off curve between the roughness of deformation distribution and the NSSD with smoothing factor variation (Figure 2). Based on the trade-off curve, we chose the optimum smoothing

factor of 0.19 to obtain the best solution of the distribution of reservoir deformations in this case (Figure 3a).
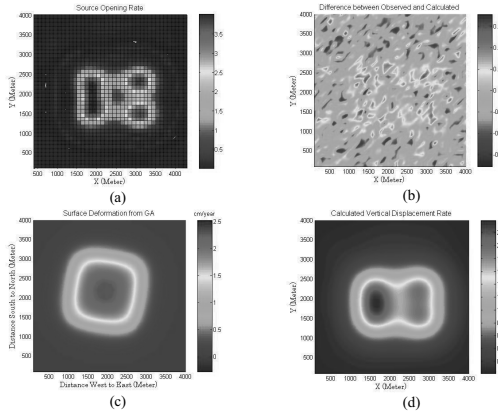

Figure 3. (a) The best modeled reservoir deformation, (b) Residual between the calculated and observed surface defomation, (c) and (d) Surface deformation from forward modeling of GA and least square inversion, respectively, (unit in cm/year).

In order to evaluate the performance of this inversion, we forwarded the inversion results to obtain surface uplift maps. The calculated surface uplift map (Figure 3d) is closed to the synthetic model one in Figure 1b. A residual map between the synthetic model and the calculated surface uplift is shown in Figure 3b. It is comparable to the input of noise in the synthetic model (Figure 1c). RMSE with the optimum smoothing factor of 0.19 is 0.114 cm, and it is comparable to the standard deviation of the additive noise 0.100 cm. The RMSE with the optimum smoothing factor is 0.114 cm, meanwhile the standard deviation of the additive noise is 0.100 cm. These errors are comparable; therefore this approach is acceptable and we can apply it to the real data of the oil sand field.

REAL DATA

InSAR deformation map estimated by the stacking technique from six interferograms was inverted by the proposed two-step inversion method. Figure 4a shows the observed vertical surface displacement map and Figure 4b shows the modeled vertical surface displacement map which was estimated by GA inversion at the first step. We constrained the lower and upper bounds of length, width, depth, chamber development and strike of the dislocation plane (considered as steam chamber in this case) to 800-3,000 m, 800-3,000 m, 200-300 m, 0-1 m and 0°-360°, respectively in search space. We also considered the dip angle of zero as one of the inversion parameters and used the initial population of 800 individuals and a number of generations are 500. After all parents had been paired off from selected population, a random

number between 0 and 1 was generated. This random number was compared to a specified crossover probability of 0.7. If the number was less than the crossover probability, the two parents were crossed over. Position of crossover in which part of the right crossover bit-string is exchanged between parents was also randomly selected along the bit-string representation.
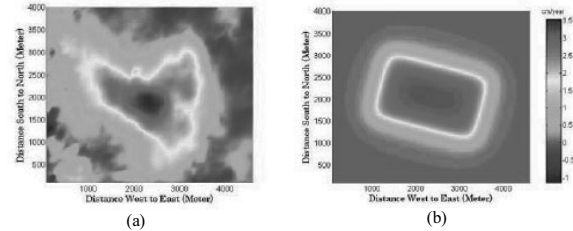

Figure 4. (a) Observed surface vertical displacement from InSAR data, (b) Modeled vertical surface displacement from GA.

Like crossover operation, mutation also needed probability to maintain some random character in the search process. We specified the mutation probability of 0.4; therefore, if a random number is less than the mutation probability, a tested bit was flipped in parity. From the genetic algorithm, we obtained the best-fit model predicted the rectangular dislocation plane with length, width and depth of 2,413 m, 1,533 m and 297 m, respectively with RMSE of 0.627 cm. The depth of deformation source is in good agreement with real data related to the depth of injection wells.
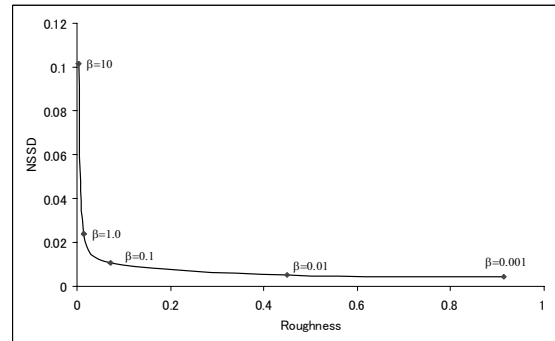

Figure 5. Trade-off curve between roughness and NSSD of solution for real data.

To estimate the detailed deformation of the reservoir from observed-surface-uplift data based on the SAR interferometry measurement, we used a penalty function technique in least square inversion as the second step of our approach (Du et al. 1992). The best-fit-single dislocation plane model from the genetic algorithm inversion was enlarged to a 4.6 x 4.0 km horizontal dislocation plane. The enlarged-dislocation plane was then discretized into 100 x 100 m patches for the inversion of distributed-source deformation. This

deformation is interpreted as steam-chamber development under SAGD process. In this study, we used the penalty function technique with five smoothing factors, i.e. 0.001, 0.01, 0.1, 1, and 10. Based on analysis of trade-off curve between roughness and NSSD in Figure 5, the source deformation rate (Figure 6a) is the best solution with smoothing factor of 0.1. For the lowest smoothing factor (0.001) the reservoir vertical deformation rate is highly oscillatory. For the highest smoothing factor (10), however, the reservoir vertical deformation is overly smooth. The reservoir deformation pattern in Figure 6a is closely related to well pair locations in Figure 6d.
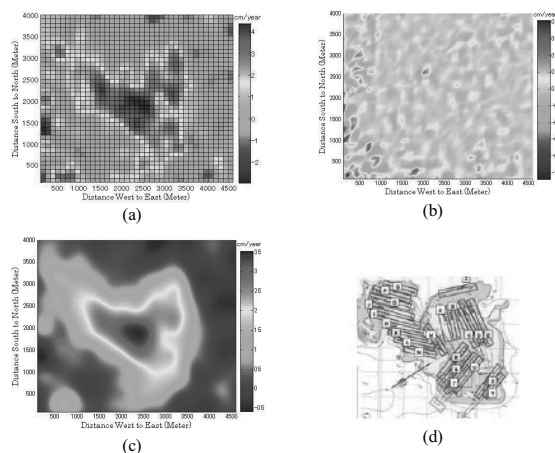

Figure 6. (a) Modeled reservoir deformation map with smoothing factor 0.1, (b) residual between the modeled and observed surface uplift, (c) surface uplift from forward modeling, and (d) configuration of production and injection well (JACOS, 2009).

The map of modeled surface displacement (Figure 6c) is comparable to the observed uplift in Figure 4a in which has a root-mean-square error of 0.125. Figur 6b is a residual map between the calculated and observed surface uplift. Small residuals between observed and modeled displacements may be related to some noises in InSAR data, especially atmospheric artifacts. Furthermore, a map of volume change at each grid point can be obtained by multiplication the grid size and vertical reservoir deformation in each corresponding grid. Finally, we obtain that the total of volume change rate is 150,809 m^3 a year by summation of individual volume change.. This volume change rate is considered as steam chamber growth during SAGD process.

CONCLUSIONS

In this paper, in order to evaluate the deformation of the oil sand reservoir caused by steam injections, we proposed the two-step inversion approach of InSAR data consisting of the genetic algorithms and least-squares method. We applied the genetic algorithm for estimating the rough reservoir deformation based on surface vertical uplifts. The result shows that the depth of the target reservoir is in good agreement with the injected point at borehole. We then applied the penalty function technique in the least square inversion with the smoothing factor to estimate the best vertical deformation rate. Based on this technique, the vertical deformation distribution demonstrates a good agreement with the well pair configuration. Finally, we estimated the total volume change rate of 150,809 m^3 a year that corresponds with the growth of the steam chambers.

REFERENCES

Burgmann, R., Rosen, P.A., and Fielding, E.J., 2000, Synthetic Aperture Radar Interferometry to measure earth`s surface topography and its deformation, *Annu. Rev. Earth Planet, Sci*., **28**, 169-209.
Du, Y., Aydin, A., and Segall, P., 1992, Comparison of various inversion techniques as applied to the determination of a geophysical deformation model for the 1983 Borah Peak earthquake, *Bulletin of the Seismological Society America*, **82**, 1840-1866.
JACOS, 2009, Hangingstone Demontration Project 2008: Thermal In-Situ Scheme Progress Report, Approval No. 8788G, presented on March 23, 2009.
Klees, R., and Massonnet, D., 1999, Deformation measurements using SAR interferometry: potential and limitations, *Geologie enMinjbouw*, **77**, 161-176.
Mathieson, A., Wright, I., Roberts, D., and Ringrose, P., 2009, Satellite imaging to monitor CO2 movement at Krechba, *Algeria. Energy Procedia*. **1**, 2201-2209.
Okada, Y., 1985, Surface deformation due to shear and tensile faults in a half space, *Bulletin of the Seismological Society America*, **75**, 1135-1154.
Patzek, T.W., and Silin, D.B., 2000, Use of INSAR in surveillance and control of a large field project, *Lawrence Berkeley National Laboratory*.
Patzek, T.W., Silin, D.B., and Fielding, E., 2001, Use of satellite radar images radar images in surveillance and control to two giant oilfields in California, SPE *Annual Technical Orleans*, 30 September – 3 October.